PERGAMON

International Journal of Heat and Mass Transfer 45 (2002) 2967–2981

International Journal of HEAT and MASS TRANSFER

www.elsevier.com/locate/ijhmt

Natural convection in a shallow cylindrical annuli

D.M. Leppinen

Department of Applied Mathematics and Theoretical Physics, University of Cambridge, Silver Street, Cambridge CB3 9EW, UK

Received 20 September 1999; received in revised form 3 January 2002

Abstract

This paper examines natural convection in the shallow annular gap between two concentric circular cylinders. Asymptotic solutions are obtained in the limit as the aspect ratio ϵ (defined as the ratio of the enclosure height to the gap width) goes to 0. It is shown that the solution at $O(\epsilon^n)$ can only be completely specified by examining the governing equations at $O(\epsilon^{n+2})$. Solutions are obtained, and Nusselt number correlations are presented, when the dimensionless radius of the inner cylinder δ is of $O(1/\epsilon)$ and when δ is of $O(1)$. The results indicate that curvature effects profoundly influence the nature of convection in shallow annular enclosures.

1. Introduction

Cormack, Leal and Imberger [1] (hereafter referred to as CLI) used asymptotic analysis to examine natural convection in a shallow rectangular cavity due to differentially heated end walls. In particular, CLI examined the case where the upper and lower boundaries were perfectly insulating and where the height of the cavity was much less than the distance between the hot and cold end walls. CLI showed that the flow can be divided into a central core region and two end zone regions. In the central core the flow is parallel with fluid travelling towards the cold end wall in the upper half of the cavity and fluid travelling towards the hot wall in the lower half of the cavity. The flow is symmetrically turned through 180° in the approximately square end zone regions. At leading order, CLI showed that the temperature varies linearly between the hot and cold end walls. The key features of the asymptotic analysis performed by CLI has been verified numerically [2] and experimentally [3].

The purpose of this paper is to extend the analysis of CLI to the case of convection in a shallow annular gap between two concentric circular cylinders maintained at different temperatures. The objective is to examine the influence of curvature on the nature of convection in shallow enclosures. The term curvature is used here to highlight the fact that in a cylindrical annulus the heat transfer area increases in proportion to the radius when moving from the inner cylinder to the outer cylinder, whereas in a rectangular cavity the heat transfer area is constant when moving from the hot end wall to the cold end wall. It has previously been noted by de Vahl Davis and Thomas [4] that curvature effects strongly influence the nature of convection in tall cylindrical annuli.

Merker and Leal [5] (hereafter referred to as ML) were the first to examine natural convection in shallow cylindrical annuli. They suggested this as a model for the circulation patterns in shallow lakes resulting from a localized source of heat. ML used the same techniques as CLI and examined the convection by dividing the domain into a central core region and two end zone regions near the inner and outer cylinders. During the course of their analysis, ML make various assumptions based on the results obtained by CLI. Not all of the assumptions made by ML are valid, however, and a revised version of the asymptotic analysis for natural convection in shallow cylindrical annuli is presented in this paper.

2. Mathematical model

A cross-section of the annular enclosure considered in this paper is given in Fig. 1. The radius of the inner cylinder is r_1 and the radius of the outer cylinder is $r_2 = r_1 + \ell$. The height of the enclosure is h and the aspect ratio is $\epsilon = h/\ell$. For the shallow enclosures of interest here $\epsilon \ll 1$. A measure of curvature in the annular gap is given by $\Gamma = r_1/\ell$, and as $\Gamma \to \infty$ the annular gap approaches the two-dimensional cavity studied by CLI.

0017-9310/02/$ - see front matter
PII: S0017-9310(02)00020-0

Nomenclature

c_n, d_n	numerical constants when $\Gamma \sim O(1)$
c_n^k, d_n^k	numerical constants when $\delta \sim O(1)$
c_p	specific heat capacity at constant pressure
C_n^k, D_n^k	numerical constants when $\delta \sim O(1)$
Gr	Grashof number of cylindrical enclosure, $Gr = g\alpha(T_1 - T_2)h^3/\nu^2$
g	coefficient of gravity
h	height of annular gap
k	thermal conductivity
ℓ	distance between inner and outer cylinder, $\ell = r_2 - r_1$
Nu	Nusselt number
p^*	thermodynamic pressure
P^*	reduced pressure, $P^* = p^* - \rho_0 g z^*$
Pr	Prandtl number, $Pr = \nu/\kappa$
r	dimensionless radial coordinate, $r = r^*/h$
$r_1(r_2)$	radius of inner (outer) cylinder
T^*	temperature
$T_1(T_2)$	temperature of inner (outer) cylinder
u	dimensionless radial velocity, $u = u^*/(g\alpha h^3(T_1 - T_2)/\nu\ell)$
v	dimensionless vertical velocity, $v = v^*/(g\alpha h^3(T_1 - T_2)/\nu\ell)$
x	dimensionless displacement from inner cylinder, $x = r - \delta$
z	dimensionless vertical coordinate, $z = z^*/h$

Greek symbols

α	thermal expansion coefficient
Γ	curvature parameter, $\Gamma = r_1/\ell$
δ	dimensionless radius of inner cylinder, $\delta = r_1/h$
ϵ	aspect ratio of annular gap, $\epsilon = h/\ell$
η	stretched asymptotic matching variable, $\eta = \epsilon^\chi r$
θ	dimensionless temperature, $\theta = (T^* - T_2)/(T_1 - T_2)$
θ_c	conduction temperature profile defined by Eq. (60)
κ	thermal diffusivity
λ	logarithmic temperature profile parameter, $\lambda = 1/\ln(\epsilon\delta/(1+\epsilon\delta))$
ν	kinematic viscosity
ξ	displacement from outer cylinder, $\xi = r - 1/\epsilon - \delta$
ρ_0	reference density of Boussinesq system
ϕ	perturbed temperature, $\phi = \theta - \theta_c$
χ	stretching factor used during asymptotic matching
ψ	cylindrical stream function
ω	vorticity

Superscripts

*	dimensional variable
$\tilde{}$	hot end region variable
$\bar{}$	cold end region variable
$\hat{}$	core region variable

A third geometric parameter of the enclosure is $\delta = r_1/h$ which is related to ϵ and Γ by $\Gamma = \epsilon\delta$. The inner cylinder is maintained at a constant temperature T_1 and the outer cylinder is maintained at a constant temperature T_2 and it is assumed that $T_2 > T_1$. The top and bottom boundaries are assumed to be perfectly insulating and all surfaces are rigid no slip boundaries. The flow is assumed to be axisymmetric.

The governing equations are the Boussinesq form of the Navier–Stokes equations, along with the continuity equation and a conservation of thermal energy equation. The steady-state form of these equations in cylindrical coordinates is given by

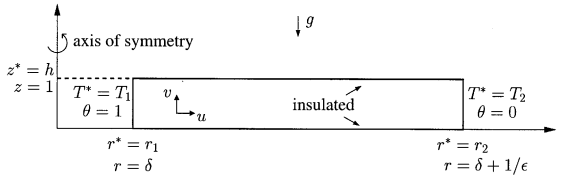

Fig. 1. Schematic of annular enclosure.

$$u^*\frac{\partial u^*}{\partial r^*} + v^*\frac{\partial u^*}{\partial z^*} = -\frac{1}{\rho_0}\frac{\partial P^*}{\partial r^*} + \nu\left(\frac{\partial^2 u^*}{\partial r^{*2}} + \frac{1}{r^*}\frac{\partial u^*}{\partial r^*} - \frac{u^*}{r^{*2}} + \frac{\partial^2 u^*}{\partial z^{*2}}\right), \tag{1}$$

$$u^*\frac{\partial v^*}{\partial r^*} + v^*\frac{\partial v^*}{\partial z^*} = -\frac{1}{\rho_0}\frac{\partial P^*}{\partial z^*} + \nu\left(\frac{\partial^2 v^*}{\partial r^{*2}} + \frac{1}{r^*}\frac{\partial v^*}{\partial r^*} + \frac{\partial^2 v^*}{\partial z^{*2}}\right) - g\alpha(T^* - T_2), \tag{2}$$

$$\frac{1}{r^*}\frac{\partial}{\partial r^*}(r^* u^*) + \frac{\partial v^*}{\partial z^*} = 0 \tag{3}$$

and

$$u^*\frac{\partial T^*}{\partial r^*} + v^*\frac{\partial T^*}{\partial z^*} = \kappa\left(\frac{\partial^2 T^*}{\partial r^{*2}} + \frac{1}{r^*}\frac{\partial T^*}{\partial r^*} + \frac{\partial^2 T^*}{\partial z^{*2}}\right). \tag{4}$$

In the above, u^* and v^* are the radial and axial velocities, respectively, T^* is temperature, $P^* = p^* - \rho_0 g z^*$ is the reduced pressure where p^* is the thermodynamic pressure, ρ_0 is the reference density, and g is the acceleration due to gravity. The reference density has been chosen to

correspond to the fluid density at the temperature T_2 of the outer cylinder. Gravity acts downwards parallel to the axis of rotational symmetry. The kinematic viscosity ν, the thermal diffusivity κ and the coefficient of thermal expansion α are all assumed to be constant.

Eqs. (1)–(4) are nondimensionalized using

$$r=\frac{r^*}{h},\quad z=\frac{z^*}{h},\quad \theta=\frac{T^*-T_2}{T_1-T_2},$$
$$u=\frac{u^*}{g\alpha h^3(T_1-T_2)/\nu\ell}\quad\text{and}\quad v=\frac{v^*}{g\alpha h^3(T_1-T_2)/\nu\ell},$$

where θ is the nondimensional temperature. This is the same nondimensionalization used by CLI and ML and it is used here to facilitate comparison with the previous work.

With the introduction of the axisymmetric stream function ψ, and vorticity ω, defined by the relations

$$\omega=\frac{\partial u}{\partial z}-\frac{\partial v}{\partial r},\quad u=-\frac{1}{r}\frac{\partial\psi}{\partial z}\quad\text{and}\quad v=\frac{1}{r}\frac{\partial\psi}{\partial r},\tag{5}$$

the governing equations can be reduced to

$$\frac{Gr\epsilon^2}{r}\left(\frac{\partial\psi}{\partial r}\frac{\partial\omega}{\partial z}-\frac{\partial\psi}{\partial z}\frac{\partial\omega}{\partial r}+\frac{\omega}{r}\frac{\partial\psi}{\partial z}\right)=\epsilon\left(\frac{\partial^2\omega}{\partial r^2}+\frac{1}{r}\frac{\partial\omega}{\partial r}-\frac{\omega}{r^2}+\frac{\partial^2\omega}{\partial z^2}\right)-\frac{\partial\theta}{\partial r},\tag{6}$$

$$\frac{1}{r}\frac{\partial^2\psi}{\partial r^2}-\frac{1}{r^2}\frac{\partial\psi}{\partial r}+\frac{1}{r}\frac{\partial^2\psi}{\partial z^2}=-\omega\tag{7}$$

and

$$\frac{GrPr\epsilon}{r}\left(\frac{\partial\psi}{\partial r}\frac{\partial\theta}{\partial z}-\frac{\partial\psi}{\partial z}\frac{\partial\theta}{\partial r}\right)=\frac{\partial^2\theta}{\partial r^2}+\frac{1}{r}\frac{\partial\theta}{\partial r}+\frac{\partial^2\theta}{\partial z^2}.\tag{8}$$

The nondimensional boundary conditions are

$$\psi=\frac{\partial\psi}{\partial r}=0,\quad \theta=1\ \text{ at }\ r=\delta,\tag{9}$$

$$\psi=\frac{\partial\psi}{\partial r}=\theta=0\ \text{ at }\ r=\delta+\frac{1}{\epsilon}\tag{10}$$

and

$$\psi=\frac{\partial\psi}{\partial z}=\frac{\partial\theta}{\partial z}=0\ \text{ at }\ z=0,1.\tag{11}$$

In the above, Pr is the Prandtl number defined by $Pr=\nu/\kappa$ and Gr is the Grashof number defined by $Gr=g\alpha(T_1-T_2)h^3/\nu^2$.

In this paper the solution of Eqs. (6)–(8) subject to boundary conditions (9)–(11) will be obtained in the asymptotic limit as $\epsilon\to 0$ with both Gr and Pr fixed. As noted previously by ML there are two cases of interest. The first case is the limit as $\epsilon\to 0$ with Γ of O(1). In this case δ, the radius of the inner cylinder, is of $O(1/\epsilon)$. The second case is the limit as $\epsilon\to 0$ with δ of O(1) so that Γ is of $O(\epsilon)$. In both cases the solution technique involves using matched asymptotic expansions in order to match end region solutions near the inner and outer cylinders, to central core region solutions where radial changes take place over distances of $O(1/\epsilon)$.

3. The limit as $\epsilon\to 0$ with Γ of O(1)

When Γ is of O(1), the radial coordinate r is of $O(1/\epsilon)$ throughout the entire annular cavity and following ML it is convenient to make the transformation $r=\delta+x$, so that $1/r=1/(\delta+x)=\epsilon/(\Gamma+\epsilon x)$ with x varying from $x=0$ at the inner cylinder to $x=1/\epsilon$ at the outer cylinder. The transformed equations become

$$\frac{Gr\epsilon^3}{\Gamma+\epsilon x}\left(\frac{\partial\psi}{\partial x}\frac{\partial\omega}{\partial z}-\frac{\partial\psi}{\partial z}\frac{\partial\omega}{\partial x}+\frac{\epsilon\omega}{\Gamma+\epsilon x}\frac{\partial\psi}{\partial z}\right)=-\frac{\partial\theta}{\partial x}+\epsilon\left(\frac{\partial^2\omega}{\partial x^2}+\frac{\partial^2\omega}{\partial z^2}\right)+\frac{\epsilon^2}{\Gamma+\epsilon x}\left(\frac{\partial\omega}{\partial x}-\frac{\epsilon\omega}{\Gamma+\epsilon x}\right),\tag{12}$$

$$\frac{\epsilon}{\Gamma+\epsilon x}\left(\frac{\partial^2\psi}{\partial x^2}-\frac{\epsilon}{\Gamma+\epsilon x}\frac{\partial\psi}{\partial x}+\frac{\partial^2\psi}{\partial z^2}\right)=-\omega\tag{13}$$

and

$$\frac{GrPr\epsilon^2}{\Gamma+\epsilon x}\left(\frac{\partial\psi}{\partial x}\frac{\partial\theta}{\partial z}-\frac{\partial\psi}{\partial z}\frac{\partial\theta}{\partial x}\right)=\frac{\partial^2\theta}{\partial x^2}+\frac{\epsilon}{\Gamma+\epsilon x}\frac{\partial\theta}{\partial x}+\frac{\partial^2\theta}{\partial z^2}.\tag{14}$$

3.1. Core region solutions

In the central core region radial changes occur over distances of $O(1/\epsilon)$ which suggests the introduction of a core variable $\hat{x}=\epsilon x$. If θ, ψ and ω are denoted by $\hat{\theta}$, $\hat{\psi}$ and $\hat{\omega}$ in the central core, the governing equations become

$$\frac{Gr\epsilon^2}{\Gamma+\hat{x}}\left(\frac{\partial\hat{\psi}}{\partial\hat{x}}\frac{\partial\hat{\omega}}{\partial z}-\frac{\partial\hat{\psi}}{\partial z}\frac{\partial\hat{\omega}}{\partial\hat{x}}+\frac{\hat{\omega}}{\Gamma+\hat{x}}\frac{\partial\hat{\psi}}{\partial z}\right)=-\frac{\partial\hat{\theta}}{\partial\hat{x}}+\frac{\partial^2\hat{\omega}}{\partial z^2}+\epsilon^2\left(\frac{\partial^2\hat{\omega}}{\partial\hat{x}^2}+\frac{1}{\Gamma+\hat{x}}\frac{\partial\hat{\omega}}{\partial\hat{x}}-\frac{\hat{\omega}}{(\Gamma+\hat{x})^2}\right),\tag{15}$$

$$\frac{1}{\Gamma+\hat{x}}\frac{\partial^2\hat{\psi}}{\partial z^2}+\frac{\epsilon^2}{\Gamma+\hat{x}}\left(\frac{\partial^2\hat{\psi}}{\partial\hat{x}^2}-\frac{1}{\Gamma+\hat{x}}\frac{\partial\hat{\psi}}{\partial\hat{x}}\right)=-\omega\tag{16}$$

and

$$\frac{GrPr\epsilon^2}{\Gamma+\hat{x}}\left(\frac{\partial\hat{\psi}}{\partial\hat{x}}\frac{\partial\hat{\theta}}{\partial z}-\frac{\partial\hat{\psi}}{\partial z}\frac{\partial\hat{\theta}}{\partial\hat{x}}\right)=\frac{\partial^2\hat{\theta}}{\partial z^2}+\epsilon^2\left(\frac{\partial^2\hat{\theta}}{\partial\hat{x}^2}+\frac{1}{\Gamma+\hat{x}}\frac{\partial\hat{\theta}}{\partial\hat{x}}\right),\tag{17}$$

where the rescaling $\hat{\psi}=\epsilon\psi$ has been used to ensure a balance at leading order in the stream function equation.

Since it will be shown that streamlines from the core region eventually enter the end regions this same scaling for ψ will have to be used in the end regions. A solution to these equations is sought using a regular asymptotic expansion of the form

$$\left(\hat{\theta},\hat{\psi},\hat{\omega}\right)=\sum_{i=0}^{N}\epsilon^{i}\left(\hat{\theta}_i,\hat{\psi}_i,\hat{\omega}_i\right). \tag{18}$$

The only boundary conditions available in the core region are $\hat{\psi}=\partial\hat{\psi}/\partial z=\partial\hat{\theta}/\partial z=0$ when $z=0$, 1.

Substituting expansion (18) into Eqs. (15)–(17) gives

$$\frac{\partial\hat{\theta}_0}{\partial\hat{x}}=\frac{\partial^2\hat{\omega}_0}{\partial z^2}, \tag{19}$$

$$\frac{1}{\Gamma+\hat{x}}\frac{\partial^2\hat{\psi}_0}{\partial z^2}=-\hat{\omega}_0 \tag{20}$$

and

$$\frac{\partial^2\hat{\theta}_0}{\partial z^2}=0 \tag{21}$$

at leading order. The solution which satisfies the boundary conditions $\partial\hat{\theta}_0/\partial z=\partial\hat{\psi}_0/\partial z=\hat{\psi}_0=0$ when $z=0$, 1 is

$$\frac{\partial\hat{\theta}_0}{\partial\hat{x}}=\frac{c_0}{\Gamma+\hat{x}}, \tag{22}$$

$$\hat{\psi}_0=-c_0\left(\frac{z^4}{24}-\frac{z^3}{12}+\frac{z^2}{24}\right) \tag{23}$$

and

$$\hat{\omega}_0=\frac{c_0}{\Gamma+\hat{x}}\left(\frac{z^2}{2}-\frac{z}{2}+\frac{1}{12}\right), \tag{24}$$

where c_0 is an undetermined function of $\hat{x}$. Eq. (21) and the boundary conditions imply that $\partial\hat{\theta}_0/\partial z=0$ and for convenience this constraint has be written in the form of Eq. (22).

At this point ML make the assumption that the flow in the core is parallel at leading order which requires the undetermined function c_0 to be a numerical constant. While this assumption is indeed true, the assumption itself is unnecessary and should not be made. It will be proven below that c_0 is indeed a numerical constant.

At $O(\epsilon)$ the governing equations and boundary conditions are identical to those at O(1). Thus the solution is given by Eqs. (22)–(24) with the subscript 0 replaced everywhere with 1.

At $O(\epsilon^2)$ the energy equation is

$$\begin{aligned}&\frac{GrPr}{\Gamma+\hat{x}}\left(\frac{\partial\hat{\psi}_0}{\partial\hat{x}}\frac{\partial\hat{\theta}_0}{\partial z}-\frac{\partial\hat{\psi}_0}{\partial z}\frac{\partial\hat{\theta}_0}{\partial\hat{x}}\right)\\&\quad=\frac{\partial^2\hat{\theta}_0}{\partial\hat{x}^2}+\frac{1}{\Gamma+\hat{x}}\frac{\partial\hat{\theta}_0}{\partial\hat{x}}+\frac{\partial^2\hat{\theta}_2}{\partial z^2},\end{aligned} \tag{25}$$

which, upon substitution of the O(1) solution, becomes

$$\frac{GrPr(c_0)^2}{(\Gamma+\hat{x})^2}\left(\frac{z^3}{6}-\frac{z^2}{4}+\frac{z}{12}\right)=\frac{1}{\Gamma+\hat{x}}\frac{\partial c_0}{\partial\hat{x}}+\frac{\partial^2\hat{\theta}_2}{\partial z^2}. \tag{26}$$

This equation is integrated from $z=0$ to $z=1$ to give

$$\frac{1}{\Gamma+\hat{x}}\frac{\partial c_0}{\partial\hat{x}}=0, \tag{27}$$

which shows that c_0 is indeed a constant and consequently Eq. (22) can be integrated to give

$$\hat{\theta}_0=c_0\ln(\Gamma+\hat{x})+d_0, \tag{28}$$

where both c_0 and d_0 are constants which can only be determined by matching the core solution with solutions in the end regions. (Repeating the above procedure at $O(\epsilon^3)$ will reveal that $\hat{\theta}_1=c_1\ln(\Gamma+\hat{x})+d_1$, where c_1 and d_1 are numerical constants.)

With the aid of Eq. (27), Eq. (25) can be integrated twice with respect to z to give

$$\hat{\theta}_2=\frac{GrPr(c_0)^2}{(\Gamma+\hat{x})^2}\left(\frac{z^5}{120}-\frac{z^4}{48}+\frac{z^3}{72}\right)+\Theta_2(\hat{x}), \tag{29}$$

where $\Theta_2(\hat{x})$ is an undetermined function of $\hat{x}$ which can only be determined by examining the energy equation at $O(\epsilon^4)$. Upon substitution of known values, the energy equation at $O(\epsilon^4)$ is given by

$$\begin{aligned}&\frac{-2(GrPr)^2(c_0)^3}{(\Gamma+\hat{x})^4}\left(\frac{z^5}{120}-\frac{z^4}{48}+\frac{z^3}{72}\right)\left(\frac{z^3}{6}-\frac{z^2}{4}+\frac{z}{12}\right)\\&\quad-\frac{GrPr}{(\Gamma+\hat{x})}\frac{\partial\hat{\psi}_0}{\partial z}\frac{\partial\Theta_2}{\partial\hat{x}}-\frac{c_1GrPr}{(\Gamma+\hat{x})^2}\frac{\partial\hat{\psi}_1}{\partial z}-\frac{c_0GrPr}{(\Gamma+\hat{x})^2}\frac{\partial\hat{\psi}_2}{\partial z}\\&\quad=\frac{4GrPr(c_0)^2}{(\Gamma+\hat{x})^4}\left(\frac{z^5}{120}-\frac{z^4}{48}+\frac{z^3}{72}\right)+\frac{\partial^2\Theta_2}{\partial\hat{x}^2}\\&\qquad+\frac{1}{\Gamma+\hat{x}}\frac{\partial\Theta_2}{\partial\hat{x}}+\frac{\partial^2\hat{\theta}_4}{\partial z^2}.\end{aligned} \tag{30}$$

Integrating Eq. (30) from $z=0$ to $z=1$ and imposing the relevant boundary conditions yields

$$\frac{\partial^2\Theta_2}{\partial\hat{x}^2}+\frac{1}{\Gamma+\hat{x}}\frac{\partial\Theta_2}{\partial\hat{x}}=\frac{4(GrPr)^2(c_0)^3}{725\,760(\Gamma+\hat{x})^4}-\frac{4GrPr(c_0)^2}{1440(\Gamma+\hat{x})^4}, \tag{31}$$

which can be integrated twice with respect to $\hat{x}$ to give

$$\begin{aligned}\Theta_2(\hat{x})=c_2\ln(\Gamma+\hat{x})+d_2+\frac{(GrPr)^2(c_0)^3}{725\,760(\Gamma+\hat{x})^2}\\-\frac{GrPr(c_0)^2}{1440(\Gamma+\hat{x})^2},\end{aligned} \tag{32}$$

where c_2 and d_2 are constants which must be determined by matching with the end region solutions.

By contrast, ML specified the value of Θ_2 by assuming that $\hat{\theta}_2$ should be of the same form as the $O(\epsilon^2)$ perturbation to the temperature field in the problem studied by CLI. Using this assumption, ML incorrectly conclude that $\Theta_2(\hat{x}) = -GrPr(c_0)^2/1440(\Gamma+\hat{x})^2$.

With $\hat{\theta}_2$ determined, the vorticity and stream function equations at $O(\epsilon^2)$ can be combined and manipulated to yield

$$\frac{\partial^4\hat{\psi}_2}{\partial z^4} = \frac{2Gr(c_0)^2}{(\Gamma+\hat{x})^2}\left(\frac{z^5}{12}-\frac{5z^4}{24}+\frac{13z^3}{72}-\frac{z^2}{16}+\frac{z}{144}\right) + \frac{2GrPr(c_0)^2}{(\Gamma+\hat{x})^2}\left(\frac{z^5}{120}-\frac{z^4}{48}+\frac{z^3}{72}-\frac{1}{1440}\right) + \frac{(GrPr)^2(c_0)^3}{(\Gamma+\hat{x})^2}\frac{1}{362\,880}-c_2. \tag{33}$$

Integrating this equation four times with respect to z, and using the boundary conditions $\partial\hat{\psi}_2/\partial z = \hat{\psi}_2 = 0$ at $z = 0, 1$ gives

$$\hat{\psi}_2 = \frac{2Gr(c_0)^2}{(\Gamma+\hat{x})^2}\frac{1}{8!}\left(\frac{10}{9}z^9-5z^8+\frac{26}{3}z^7-7z^6+\frac{7}{3}z^5-\frac{1}{9}z^3\right) + \frac{2GrPr(c_0)^2}{(\Gamma+\hat{x})^2}\frac{1}{8!}\left(\frac{1}{9}z^9-\frac{1}{2}z^8+\frac{2}{3}z^7-\frac{7}{6}z^4 + \frac{11}{9}z^3-\frac{1}{3}z^2\right)+\left(\frac{(GrPr)^2(c_0)^3}{(\Gamma+\hat{x})^2}\frac{1}{362\,880}-c_2\right) \times\left(\frac{z^4}{24}-\frac{z^3}{12}+\frac{z^2}{24}\right). \tag{34}$$

While it is possible to continue the analysis to higher orders in ϵ, this shall not pursued here. Of special note however, is that the analysis has shown that for the case of a cylindrical annulus, the core region flow becomes nonparallel at $O(\epsilon^2)$. By contrast, the core region flow is parallel to all orders in ϵ in the two-dimensional cavity studied by CLI. Thus, when Γ is of O(1) as $\epsilon \to 0$, curvature is seen to have a small but noticeable effect on the flow in the core region. This observation foreshadows the difficulties which will be faced when δ is of O(1) as $\epsilon \to 0$.

3.2. End region solutions

In the hot end region near the inner cylinder θ, ψ and ω are denoted by $\tilde{\theta}$, $\tilde{\psi}$ and $\tilde{\omega}$, while in the cold end region, $\bar{\theta}$, $\bar{\psi}$ and $\bar{\omega}$ are used. Since the streamlines in the core are parallel at leading order, they must eventually enter into the end regions. Hence $\tilde{\psi}$ and $\bar{\psi}$ must be rescaled as $\tilde{\psi} = \epsilon\psi$ and $\bar{\psi} = \epsilon\psi$. The governing equations in the hot end are Eqs. (12)–(14) while the governing equations in the cold end are obtained from Eqs. (12)–(14) by performing the transformation $\xi = 1/\epsilon - x$. The variable ξ measures the distance away from the cold cylinder wall and is introduced here to facilitate matching.

In order to match the end region solutions with solutions in the core region, the flow variables are expanded as

$$\left(\tilde{\theta},\tilde{\psi},\tilde{\omega},\bar{\theta},\bar{\psi},\bar{\omega}\right) = \sum_{i=0}^{N}\epsilon^i\left(\tilde{\theta}_i,\tilde{\psi}_i,\tilde{\omega}_i,\bar{\theta}_i,\bar{\psi}_i,\bar{\omega}_i\right). \tag{35}$$

The matching conditions between the core and end region solutions are given by

$$\lim_{\hat{x}\to 0}\left(\hat{\theta},\hat{\psi},\hat{\omega}\right) \Longleftrightarrow \lim_{x\to\infty}\left(\tilde{\theta},\tilde{\psi},\tilde{\omega}\right), \tag{36}$$

$$\lim_{\hat{x}\to 1}\left(\hat{\theta},\hat{\psi},\hat{\omega}\right) \Longleftrightarrow \lim_{\xi\to\infty}\left(\bar{\theta},\bar{\psi},\bar{\omega}\right), \tag{37}$$

where the symbol $\Longleftrightarrow$ is used to indicate that the matching conditions apply in the limit as $\epsilon \to 0$.

At O(1) the governing equations in the hot end region are

$$\frac{\partial\tilde{\theta}_0}{\partial x} = 0, \tag{38}$$

$$-\frac{1}{\Gamma}\left(\frac{\partial^2\tilde{\psi}_0}{\partial x^2}+\frac{\partial^2\tilde{\psi}_0}{\partial z^2}\right) = \tilde{\omega}_0 \tag{39}$$

and

$$\frac{\partial^2\tilde{\theta}_0}{\partial x^2}+\frac{\partial^2\tilde{\theta}_0}{\partial z^2} = 0. \tag{40}$$

When Eqs. (38) and (40) are combined with the appropriate boundary conditions, it is seen that $\tilde{\theta}_0 = 1$. In the cold end region the governing equations are the same as Eqs. (38)–(40) except that Γ is replaced by $\Gamma+1$ and $\partial/\partial x$ is replaced by $-\partial/\partial\xi$. Applying the appropriate boundary conditions, the leading order temperature field in the cold end region is given by $\bar{\theta}_0 = 0$.

In order to apply conditions (36) and (37), $\hat{\theta}_0$ is expanded in terms of the end region variables resulting in

$$c_0\ln\Gamma + c_0\left(\frac{\epsilon x}{\Gamma}-\frac{1}{2}\left(\frac{\epsilon x}{\Gamma}\right)^2+\cdots\right)+d_0 \Longleftrightarrow 1 \tag{41}$$

and

$$c_0\ln(\Gamma+1) + c_0\left(-\frac{\epsilon\xi}{\Gamma+1}-\frac{1}{2}\left(\frac{\epsilon\xi}{\Gamma+1}\right)^2-\cdots\right) + d_0 \Longleftrightarrow 0, \tag{42}$$

which gives $c_0 = 1/\ln(\Gamma/(\Gamma+1))$ and $d_0 = -\ln(\Gamma+1)/\ln(\Gamma/(\Gamma+1))$. The mismatch which occurs when matching at this order has to be accounted for when matching the solutions at higher order.

With the values of c_0 and d_0 now determined, it is interesting to note that this leading order solution does

not depend on either Gr or Pr, which indicates that the flow is controlled solely by conduction and mass conservation at leading order.

At $O(\epsilon)$ the energy equation in the hot end region simplifies to

$$\frac{\partial^2\tilde{\theta}_1}{\partial x^2}+\frac{\partial^2\tilde{\theta}_1}{\partial z^2}=0 \tag{43}$$

after substituting for the known value of $\tilde{\theta}_0$. Integrating this equation from $z=0$ to $z=1$ and using the fact that $\partial\tilde{\theta}_1/\partial z=0$ when $z=0,\ 1$ yields

$$\int_0^1 \frac{\partial^2\tilde{\theta}_1}{\partial x^2}\,\mathrm{d}z=0. \tag{44}$$

Integrating this twice with respect to x, and noting that $\tilde{\theta}_1=0$ when $x=0$ gives

$$\int_0^1 \tilde{\theta}_1\,\mathrm{d}z=a_1x, \tag{45}$$

where a_1 is a constant of integration. This equation is valid everywhere in the hot end, and in particular, it is valid in the limit when the hot end approaches the core. According to the matching condition (36)

$$\tilde{\theta}_1 \Longleftrightarrow \frac{c_0x}{\Gamma}+c_1\ln\Gamma+c_1\left(\frac{\epsilon x}{\Gamma}-\frac{1}{2}\left(\frac{\epsilon x}{\Gamma}\right)^2+\cdots\right)+d_1, \tag{46}$$

where the first term is the result of the mismatch at leading order. Substituting this expansion into Eq. (45) and retaining only the leading order terms gives

$$\frac{c_0x}{\Gamma}+c_1\ln\Gamma+d_1=a_1x. \tag{47}$$

Repeating the above analysis in the cold end region reveals

$$-\frac{c_0\xi}{\Gamma+1}+c_1\ln(\Gamma+1)+d_1=a_2\xi, \tag{48}$$

where a_2 is an undetermined constant. Combining Eqs. (47) and (48) gives $a_1=c_0/\Gamma$, $a_2=-c_0/(\Gamma+1)$ and $c_1=d_1=0$. Thus there is no additional mismatch at this order, and the end region solutions are seen to be $\tilde{\theta}_1=c_0x/\Gamma$ and $\bar{\theta}_1=-c_0\xi/(\Gamma+1)$.

At $O(\epsilon^2)$ the energy equation in the hot end region can be written as

$$\frac{\partial^2\tilde{\theta}_2}{\partial x^2}+\frac{\partial^2\tilde{\theta}_2}{\partial z^2}=-\frac{GrPrc_0}{\Gamma^2}\frac{\partial\tilde{\psi}_0}{\partial z}-\frac{c_0}{\Gamma^2} \tag{49}$$

by first substituting for the known values of $\tilde{\theta}_0$ and $\tilde{\theta}_1$. Integrating Eq. (49) from $z=0$ to $z=1$ and applying the appropriate boundary conditions yields

$$\int_0^1 \frac{\partial^2\tilde{\theta}_2}{\partial x^2}\,\mathrm{d}z=-\frac{c_0}{\Gamma^2}. \tag{50}$$

Integrating Eq. (50) twice with respect to x and applying the boundary conditions yields

$$\int_0^1 \tilde{\theta}_2\,\mathrm{d}z=-\frac{c_0}{2\Gamma^2}x^2+a_3x, \tag{51}$$

where a_3 is a constant of integration. The matching condition for $\tilde{\theta}_2$ is

$$\tilde{\theta}_2 \Longleftrightarrow -\frac{c_0}{2\Gamma^2}x^2+c_2\ln\Gamma+d_2+\frac{GrPr(c_0)^2}{\Gamma^2}\times\left(\frac{z^5}{120}-\frac{z^4}{48}+\frac{z^3}{72}-\frac{1}{1440}\right)+\frac{(GrPr)^2(c_0)^3}{725\,760\Gamma^2} \tag{52}$$

as $x\to\infty$, where the x^2 term is the result of the mismatch at leading order, and higher order terms in ϵ in the expansion of $\hat{\theta}_2$ have not been retained. Applying this matching condition with Eq. (51) yields

$$-\frac{c_0}{2\Gamma^2}x^2+c_2\ln\Gamma+d_2+\frac{(GrPr)^2(c_0)^3}{725\,760\Gamma^2}=-\frac{c_0}{2\Gamma^2}x^2+a_3x. \tag{53}$$

When the same analysis is repeated in the cold end region, the corresponding result is

$$-\frac{c_0}{2(\Gamma+1)^2}\xi^2+c_2\ln(\Gamma+1)+d_2+\frac{(GrPr)^2(c_0)^3}{725\,760(\Gamma+1)^2}=-\frac{c_0}{2(\Gamma+1)^2}\xi^2+a_4\xi. \tag{54}$$

Combining the above two equations gives $a_3=a_4=0$ as well as

$$c_2=\frac{(GrPr)^2(c_0)^3}{725\,760}\left(\frac{1}{(\Gamma+1)^2}-\frac{1}{\Gamma^2}\right)\Big/\ln\left(\frac{\Gamma}{\Gamma+1}\right) \tag{55}$$

and

$$d_2=\frac{(GrPr)^2(c_0)^3}{725\,760}\left(\frac{\ln\Gamma}{(\Gamma+1)^2}-\frac{\ln(\Gamma+1)}{\Gamma^2}\right)\Big/\ln\left(\frac{\Gamma+1}{\Gamma}\right). \tag{56}$$

With c_2 and d_2 known, the core solution has been completely determined to $O(\epsilon^2)$ and this solution will be used in Section 5 to determine the total rate of heat transfer (and hence the Nusselt number) between the hot inner cylinder and the cold outer cylinder.

At this point it would be possible to write equations to explicitly solve for $(\tilde{\psi}_0,\tilde{\psi}_1,\tilde{\psi}_2,\tilde{\theta}_2)$ and $(\bar{\psi}_0,\bar{\psi}_1,\bar{\psi}_2,\bar{\theta}_2)$ however this shall not be pursued here other then to mention that the equations and their solution technique are essentially equivalent to the corresponding equations derived and solved numerically by CLI for the case of natural convection in a shallow rectangular cavity.

4. The limit as $\epsilon \to 0$ with δ of O(1)

The asymptotic analysis when δ is of O(1) is considerably more difficult than when Γ is of O(1). The difficulty results from differences in the magnitude of curvature effects within the enclosure since when δ is of O(1), r varies from being of O(1) near the inner cylinder to being of $O(1/\epsilon)$ near the outer cylinder. In their original paper, ML note the difficulties associated with the asymptotic analysis when δ is of O(1), however, they incorrectly conclude that the solutions in the core region are identical to $O(\epsilon^2)$ for both the cases when δ is of O(1) and when Γ is of O(1). In this section it will be shown that curvature effects profoundly influence the asymptotic solutions when δ is of O(1) and that these solutions are indeed distinct from the solutions when Γ is of O(1).

The analysis begins by writing the governing equations for the core region and for the two end regions. In the core region the solutions will be identified with superscript "s, while in the hot end regions ~s are used and in the cold end region ¯s are used. As for the case when Γ is of O(1), the stream function is rescaled in each of the regions as $\hat{\psi} = \epsilon\psi$, $\tilde{\psi} = \epsilon\psi$ and $\bar{\psi} = \epsilon\psi$. This rescaling of the stream function forces a rescaling of the vorticity in the hot end region of $\tilde{\omega} = \epsilon\omega$ to ensure a balance at leading order. Upon substitution of $\tilde{\psi} = \epsilon\psi$ and $\tilde{\omega} = \epsilon\omega$ into Eqs. (6)–(8), the governing equations in the hot end region become

$$\frac{Gr}{r}\left(\frac{\partial\tilde{\psi}}{\partial r}\frac{\partial\tilde{\omega}}{\partial z} - \frac{\partial\tilde{\psi}}{\partial z}\frac{\partial\tilde{\omega}}{\partial r} + \frac{\tilde{\omega}}{r}\frac{\partial\tilde{\psi}}{\partial z}\right) = \frac{\partial^2\tilde{\omega}}{\partial r^2} + \frac{1}{r}\frac{\partial\tilde{\omega}}{\partial r} - \frac{\tilde{\omega}}{r^2} + \frac{\partial^2\tilde{\omega}}{\partial z^2} - \frac{\partial\tilde{\theta}}{\partial r}, \tag{57}$$

$$\frac{1}{r}\frac{\partial^2\tilde{\psi}}{\partial r^2} - \frac{1}{r^2}\frac{\partial\tilde{\psi}}{\partial r} + \frac{1}{r}\frac{\partial^2\tilde{\psi}}{\partial z^2} = -\tilde{\omega} \tag{58}$$

and

$$\frac{GrPr}{r}\left(\frac{\partial\tilde{\psi}}{\partial r}\frac{\partial\tilde{\theta}}{\partial z} - \frac{\partial\tilde{\psi}}{\partial z}\frac{\partial\tilde{\theta}}{\partial r}\right) = \frac{\partial^2\tilde{\theta}}{\partial r^2} + \frac{1}{r}\frac{\partial\tilde{\theta}}{\partial r} + \frac{\partial^2\tilde{\theta}}{\partial z^2}. \tag{59}$$

As noted by ML, the absence of a small parameter in Eqs. (57)–(59) highlights the difficulty of the asymptotic analysis when δ is of O(1). If the analysis where performed using asymptotic expansions of the form of sum (18), then the full nonlinear vorticity, stream function and energy equations would have to be solved at each order in ϵ. To avoid having to solve the full nonlinear equations, a small parameter can be conveniently introduced into Eqs. (57) and (58) by making the substitution

$$\theta = \phi + \theta_c, \tag{60}$$

where

$$\theta_c = \frac{\ln(\epsilon r/(1+\epsilon\delta))}{\ln(\epsilon\delta/(1+\epsilon\delta))} \tag{61}$$

is the conduction temperature profile which would result in the absence of convection ($Gr = 0$). This substitution introduces the asymptotically small parameter

$$\lambda = 1\Big/\ln\left(\frac{\epsilon\delta}{1+\epsilon\delta}\right) \sim 1/\ln\epsilon \tag{62}$$

and it is motivated by the observation that the leading order temperature field for the case when Γ is of O(1) is precisely $\theta = \theta_c$. The transformed vorticity and energy equations in the hot end region become

$$\frac{Gr}{r}\left(\frac{\partial\tilde{\psi}}{\partial r}\frac{\partial\tilde{\omega}}{\partial z} - \frac{\partial\tilde{\psi}}{\partial z}\frac{\partial\tilde{\omega}}{\partial r} + \frac{\tilde{\omega}}{r}\frac{\partial\tilde{\psi}}{\partial z}\right) = \frac{\partial^2\tilde{\omega}}{\partial r^2} + \frac{1}{r}\frac{\partial\tilde{\omega}}{\partial r} - \frac{\tilde{\omega}}{r^2} + \frac{\partial^2\tilde{\omega}}{\partial z^2} - \frac{\lambda}{r} - \frac{\partial\tilde{\phi}}{\partial r} \tag{63}$$

and

$$\frac{GrPr}{r}\left(\frac{\partial\tilde{\psi}}{\partial r}\frac{\partial\tilde{\phi}}{\partial z} - \frac{\partial\tilde{\psi}}{\partial z}\frac{\partial\tilde{\phi}}{\partial r}\right) - \lambda\frac{GrPr}{r^2}\frac{\partial\tilde{\psi}}{\partial z} = \frac{\partial^2\tilde{\phi}}{\partial r^2} + \frac{1}{r}\frac{\partial\tilde{\phi}}{\partial r} + \frac{\partial^2\tilde{\phi}}{\partial z^2}. \tag{64}$$

The governing equations in the core region are obtained from Eqs. (6)–(8) by introducing the scaling $\hat{\psi} = \epsilon\psi$ and transforming the radial coordinate as $\hat{r} = \epsilon r$. Upon substituting using Eq. (60), the core region equations become

$$\frac{Gr\epsilon^2}{\hat{r}}\left(\frac{\partial\hat{\psi}}{\partial\hat{r}}\frac{\partial\hat{\omega}}{\partial z} - \frac{\partial\hat{\psi}}{\partial z}\frac{\partial\hat{\omega}}{\partial\hat{r}} + \frac{\hat{\omega}}{\hat{r}}\frac{\partial\hat{\psi}}{\partial z}\right) = \epsilon^2\left(\frac{\partial^2\hat{\omega}}{\partial\hat{r}^2} + \frac{1}{\hat{r}}\frac{\partial\hat{\omega}}{\partial\hat{r}} - \frac{\hat{\omega}}{\hat{r}^2}\right) + \frac{\partial^2\hat{\omega}}{\partial z^2} - \frac{\lambda}{\hat{r}} - \frac{\partial\hat{\phi}}{\partial\hat{r}}, \tag{65}$$

$$\epsilon^2\left(\frac{1}{\hat{r}}\frac{\partial^2\hat{\psi}}{\partial\hat{r}^2} - \frac{1}{\hat{r}^2}\frac{\partial\hat{\psi}}{\partial\hat{r}}\right) + \frac{1}{\hat{r}}\frac{\partial^2\hat{\psi}}{\partial z^2} = -\hat{\omega} \tag{66}$$

and

$$\frac{GrPr\epsilon^2}{\hat{r}}\left(\frac{\partial\hat{\psi}}{\partial\hat{r}}\frac{\partial\hat{\phi}}{\partial z} - \frac{\partial\hat{\psi}}{\partial z}\frac{\partial\hat{\phi}}{\partial\hat{r}}\right) - \lambda\epsilon^2\frac{GrPr}{\hat{r}^2}\frac{\partial\hat{\psi}}{\partial z} = \epsilon^2\left(\frac{\partial^2\hat{\phi}}{\partial\hat{r}^2} + \frac{1}{\hat{r}}\frac{\partial\hat{\phi}}{\partial\hat{r}}\right) + \frac{\partial^2\hat{\phi}}{\partial z^2}. \tag{67}$$

The governing equations in the cold end region are obtained from Eqs. (6)–(8) and (60) by using the scaling $\hat{\psi} = \epsilon\psi$ and by making the transformation $\xi = \delta + 1/\epsilon - r$.

The form of the governing equations when δ is of O(1) suggests seeking asymptotic solutions using an expansion of the form

$$(\hat{\psi},\hat{\phi},\hat{\omega}) = \sum_{i=0}^{N} \epsilon^i \left(\sum_{k=1}^{\infty} \lambda^k \left(\hat{\psi}_i^k, \hat{\theta}_i^k, \hat{\omega}_i^k \right) \right) \tag{68}$$

in the core region with identical expansions in the hot and cold end regions. In order to obtain asymptotic solutions, the inner summation must be performed before the outer summation.

Solution methodology. The objective of the analysis is to determine the first convective contribution (i.e., *Gr* number dependence) to the temperature and stream function fields in the central core region. To do this the governing equations are solved in the central core region and matched with solutions in the end regions. It will be shown that the first convective contribution in the central core region occurs at $O(\lambda^4)$. Due to the need to solve the governing equations in the hot end region numerically, matching is not performed beyond this order.

4.1. Core region solutions

The solution of the governing equations in the core region when δ is of O(1) is very similar to the solution of the governing equations when Γ is of O(1) and only the solutions will be presented here.

At $O(\lambda^k)$ the solutions are

$$\hat{\phi}_0^k = c_0^k \ln \hat{r} + d_0^k \tag{69}$$

and

$$\hat{\psi}_0^k = -(c_0^k + \delta_{1,k}) \left(\frac{z^4}{24} - \frac{z^3}{12} + \frac{z^2}{24} \right), \tag{70}$$

where c_0^k and d_0^k are unknown numerical constants which must be determined by matching with the end region solutions and $\delta_{1,k} = 1$ when $k = 1$ and $\delta_{1,k} = 0$ when $k > 1$.

At $O(\epsilon\lambda^k)$ the solutions are

$$\hat{\phi}_1^k = c_1^k \ln \hat{r} + d_1^k \tag{71}$$

and

$$\hat{\psi}_1^k = -c_1^k \left(\frac{z^4}{24} - \frac{z^3}{12} + \frac{z^2}{24} \right), \tag{72}$$

where c_1^k and d_1^k are unknown numerical constants which must be determined by matching with the end region solutions.

At $O(\epsilon^2\lambda^k)$ the solutions are

$$\hat{\phi}_2^k = c_2^k \ln \hat{r} + d_2^k + e_2^k \frac{GrPr}{\hat{r}^2} \left(\frac{z^5}{120} - \frac{z^4}{48} + \frac{z^3}{72} - \frac{1}{1440} \right) + f_2^k \left(\frac{(GrPr)^2}{\hat{r}^2} \frac{1}{725\,760} \right) \tag{73}$$

and

$$\hat{\psi}_2^k = e_2^k \frac{2GrPr}{\hat{r}^2} \frac{1}{8!} \left(\frac{1}{9} z^9 - \frac{1}{2} z^8 + \frac{2}{3} z^7 - \frac{7}{6} z^4 + \frac{11}{9} z^3 - \frac{1}{3} z^2 \right) + g_2^k \frac{2Gr}{\hat{r}^2} \frac{1}{8!} \left(\frac{10}{9} z^9 - 5z^8 + \frac{26}{3} z^7 - 7z^6 + \frac{7}{3} z^5 - \frac{1}{9} z^3 \right) + \left(\frac{2 f_2^k (GrPr)^2}{\hat{r}^2} \frac{1}{725\,760} - c_2^k \right) \left(\frac{z^4}{24} - \frac{z^3}{12} + \frac{z^2}{24} \right), \tag{74}$$

where c_2^k and d_2^k are unknown numerical constants which must be determined by matching with the end region solutions,

$$e_2^k = \delta_{1,k-1} + c_0^{k-1} + \sum_{m+n=k} c_0^m (\delta_{1,n} + c_0^n),$$

$$f_2^k = \sum_{m+n=k} e_2^m (\delta_{1,n} + c_0^n)$$

and

$$g_2^k = \sum_{m+n=k} (\delta_{1,m} + c_0^m)(\delta_{1,n} + c_0^n).$$

An examination of Eqs. (73) and (74) reveals that some of the terms in the asymptotic expansion in the core region jump order when matching with solutions in the hot end region. To accommodate this, the matching is performed using an intermediate variable $\eta = r\epsilon^\chi = \hat{r}\epsilon^{\chi-1}$, where $0 < \chi < 1$. (See Hinch [6] for details.) Matching is performed by expressing the core region solutions and the hot end region solutions in terms of η and then ensuring that the solutions have the identical form throughout the intermediate matching region (see Fig. 2). Observing that

$$\frac{\epsilon^2}{\hat{r}^2} = \frac{1}{\eta^2} \epsilon^{2\chi} = \frac{1}{r^2} \tag{75}$$

it follows that the $1/\hat{r}^2$ terms which occur at $O(\epsilon^2)$ in the core region must be matched with $1/r^2$ terms at O(1) in the hot end region. To complicate matters further it can be shown that for all $n \geqslant 1$ there are terms in the core region solutions at $O(\epsilon^{2n})$ which vary as $1/\hat{r}^{2n}$ and hence jump to O(1) when matching with solutions in the hot end region.

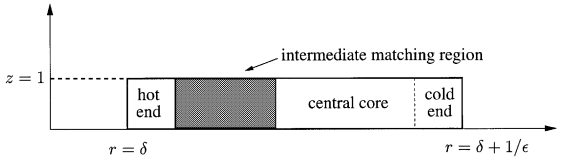

Fig. 2. Intermediate matching region when $\epsilon \to 0$ with δ of O(1).

4.2. The cold end region

The temperature matching condition between the core region and the cold end region is given by

$$\lim_{\hat{r}\to 1+\epsilon\delta} \hat{\phi}_n^k \Longleftrightarrow \lim_{\xi\to\infty} \bar{\phi}_n^k, \tag{76}$$

where it is noted that when matching with the cold end region no terms in the core region solution jump order. For the current purposes matching will only be performed for $n = 0$.

At $O(\lambda^k)$ (for all k) the energy equation in the cold end region gives

$$\frac{\partial^2 \bar{\phi}_0^k}{\partial \xi^2} + \frac{\partial^2 \bar{\phi}_0^k}{\partial z^2} = 0, \tag{77}$$

while the vorticity equation gives

$$\frac{\partial \bar{\phi}_0^k}{\partial \xi} = 0. \tag{78}$$

Combining Eqs. (77) and (78) with the boundary conditions $\partial\bar{\phi}_0^k/\partial z = 0$ when $z = 0, 1$ and $\bar{\phi}_0^k = 0$ when $\xi = 0$ requires $\bar{\phi}_0^k = 0$ for all k. The solution to the energy equation at $O(\lambda^k)$ in the core region is simply $\hat{\phi}_0^k = c_0^k \ln\hat{r} + d_0^k$. Expressing $\hat{\phi}_0^k$ in terms of ξ and applying the matching condition (76) yields

$$c_0^k \ln(1 + \epsilon(\delta - \xi)) + d_0^k \Longleftrightarrow \bar{\phi}_0^k = 0, \tag{79}$$

which can be expanded to give

$$c_0^k(\epsilon(\delta - \xi) - 1/2\epsilon^2(\delta - \xi)^2 + \cdots) + d_0^k \Longleftrightarrow 0. \tag{80}$$

Hence to leading order in ϵ, $d_0^k = 0$ for all k.

4.3. The hot end region

The energy equation in the hot end region at $O(\lambda^k)$ can be written as

$$\frac{\partial^2 \tilde{\phi}_0^k}{\partial r^2} + \frac{1}{r}\frac{\partial \tilde{\phi}_0^k}{\partial r} + \frac{\partial^2 \tilde{\phi}_0^k}{\partial z^2} = f(r,z), \tag{81}$$

where $f(r,z)$ is a forcing function, which can be written explicitly by examining Eq. (64).

The general solution to Eq. (81) is

$$\tilde{\phi}_0^k = (\tilde{\phi}_0^k)_{\mathrm{h}} + (\tilde{\phi}_0^k)_{\mathrm{nh}}, \tag{82}$$

where $(\tilde{\phi}_0^k)_{\mathrm{h}}$ is the homogeneous solution to Eq. (81) with $f(r,z)$ replaced by 0 and $(\tilde{\phi}_0^k)_{\mathrm{nh}}$ is a particular solution to nonhomogeneous Eq. (81) when $f(r,z) \neq 0$. The boundary conditions on $\tilde{\phi}_0^k$ are $\tilde{\phi}_0^k = 0$ when $r = \delta$ and $\partial\tilde{\phi}_0^k/\partial z = 0$ when $z = 0, 1$. Moreover $(\tilde{\phi}_0^k)_{\mathrm{h}}$ and $(\tilde{\phi}_0^k)_{\mathrm{nh}}$ must be of the correct form to match with solutions from the core region. Noting from Section 4.1 above that the core region solutions behave as the sum of logarithmic terms, constant terms and terms which jump order with a radial dependence of $1/r^{2n}$ in the intermediate matching region, it follows that the hot end region solutions must display the same behaviour in the intermediate matching region. The homogeneous solution to Eq. (81) which satisfies all of the boundary conditions and which is of the correct form to match with the core region solutions is simply

$$\tilde{\phi}_0^k = C_0^k \ln(r/\delta), \tag{83}$$

where C_0^k is a numerical constant which must be determined by matching. Thus, to ensure that the hot end regions solutions are of the correct form to match with the core region solutions it follows that the particular nonhomogeneous solution to Eq. (81) must behave as

$$(\tilde{\phi}_0^k)_{\mathrm{nh}} \Longleftrightarrow D_0^k + J_0^k(r,z) \tag{84}$$

throughout the intermediate matching region where D_0^k is an as of yet undetermined numerical constant and where $J_0^k(r,z)$ is used to denote the sum of terms which jump to order $O(\lambda^k)$ when matching between the core region and the hot end region.

4.3.1. The logarithmic and constant terms

Matching the logarithmic and constant terms in the core region with the corresponding terms in the hot end region and is performed using the intermediate variable $\eta = r\epsilon^\chi = \hat{r}\epsilon^{\chi-1}$, where $0 < \chi < 1$. The matching condition is

$$\sum_{k=1}^{\infty} \lambda^k \left(C_0^k \ln(r/\delta) + D_0^k\right) \Longleftrightarrow \sum_{k=1}^{\infty} \lambda^k \left(c_0^k \ln\hat{r} + d_0^k\right), \tag{85}$$

which is expanded to yield

$$\begin{aligned} &C_0^1\chi\lambda\ln(1/\epsilon) + \left(C_0^1\ln(\eta/\delta) + D_0^1\right)\lambda + C_0^2\chi\lambda^2\ln(1/\epsilon) + \cdots \\ &\quad\Longleftrightarrow c_0^1(\chi-1)\lambda\ln(1/\epsilon) + \left(c_0^1\ln\eta + d_0^1\right)\lambda \\ &\qquad + c_0^2(\chi-1)\lambda^2\ln(1/\epsilon) + \cdots. \end{aligned} \tag{86}$$

By expanding Eq. (62) in terms of ϵ as $\epsilon \to 0$ it can be shown that

$$\lambda\ln(1/\epsilon) = -1 + \lambda(\ln\delta - (\epsilon\delta) + \frac{1}{2}(\epsilon\delta)^2 - \frac{1}{3}(\epsilon\delta)^3 - \cdots). \tag{87}$$

Thus, to leading order in ϵ, $\lambda\ln(1/\epsilon) = -1 + \lambda\ln\delta$ and when this substitution is made into Eq. (86) and the coefficients of the powers of λ are compared it is seen that

$$C_0^1\chi = c_0^1(\chi - 1) \tag{88}$$

and

$$\begin{aligned} &C_0^k\ln(\eta/\delta) + D_0^k + C_0^k\chi\ln\delta - C_0^{k+1}\chi \\ &\quad = c_0^k\ln\eta + d_0^k + c_0^k(\chi-1)\ln\delta - c_0^{k+1}(\chi-1), \end{aligned} \tag{89}$$

for $k > 1$. Since Eqs. (88) and (89) must be satisfied for all values of $0 < \chi < 1$ it follows that $C_0^1 = c_0^1 = 0$, and that $C_0^k = c_0^k$ with $D_0^k = d_0^k + c_0^{k+1}$ when $k > 1$. Matching in the cold end region has shown that $d_0^k = 0$ for all k so it follows that $c_0^{k+1} = C_0^{k+1} = D_0^k$.

4.3.2. The nonhomogeneous solutions

While the above analysis has shown how the constants D_0^k are matched with solutions in the core region, the numerical value of these constants can only be determined by calculating the nonhomogeneous solutions noted in Eq. (84). The nonhomogeneous solutions are obtained using numerical integration and results are presented in this section for the particular value of $\delta = 1$.

The energy equation at $O(\lambda)$ in the hot end region is

$$\frac{\partial^2 \tilde{\phi}_0^1}{\partial r^2} + \frac{1}{r}\frac{\partial \tilde{\phi}_0^1}{\partial r} + \frac{\partial^2 \tilde{\phi}_0^1}{\partial z^2} = 0 \tag{90}$$

and the only solution which satisfies the appropriate boundary conditions and which can be matched with the core region solutions is $\tilde{\phi}_0^1 = C_0^1 \ln(r/\delta)$. (At $O(\lambda)$ there are no terms in the core region solutions which jump order.) Noting from above that $C_0^1 = 0$ it follows that $\tilde{\phi}_0^1 = 0$. Since Eq. (90) is homogeneous, it follows that there is no nonhomogeneous solution and that $D_0^1 = 0$. This in turn implies that $C_0^2 = c_0^2 = 0$ so that the homogeneous solution at $O(\lambda^2)$ vanishes.

The vorticity and stream function equations at $O(\lambda)$ can be combined to give

$$\left(\frac{\partial^2}{\partial r^2} + \frac{1}{r}\frac{\partial}{\partial r} - \frac{1}{r^2} + \frac{\partial^2}{\partial z^2}\right)\left(\frac{1}{r}\frac{\partial^2}{\partial r^2} - \frac{1}{r^2}\frac{\partial}{\partial r} + \frac{1}{r}\frac{\partial^2}{\partial z^2}\right)\tilde{\psi}_0^1 = -\frac{1}{r}. \tag{91}$$

The boundary conditions on $\tilde{\psi}_0^1$ are $\tilde{\psi}_0^1 = \partial\tilde{\psi}_0^1/\partial z = 0$ when $z = 0,\ 1$ and $\tilde{\psi}_0^1 = \partial\tilde{\psi}_0^1/\partial r = 0$ when $r = \delta$. Throughout the entire matching region, $\tilde{\psi}_0^1$ must satisfy

$$\tilde{\psi}_0^1 \Longleftrightarrow -\left(z^4/24 - z^3/12 + z^2/24\right). \tag{92}$$

Eq. (91) is clearly related to the biharmonic equation solved by CLI in relation to convection in shallow rectangular enclosures. Below it will be shown that the solution of $\tilde{\psi}_0^1$ is required in order to determine higher order approximations to $\tilde{\psi}$ and $\tilde{\phi}$, and the approach adopted here is to use a numerical technique to solve Eq. (91). CLI also employed a numerical technique to perform the matching during their asymptotic analysis and the analysis which follows is closely related to that of CLI. The solution of Eq. (91) is plotted in Fig. 3 for the specific value of $\delta = 1$. It is seen that the leading order stream function smoothly turns the flow through 180°, in a similar manner to that observed in convection in shallow rectangular enclosures (cf. CLI, Fig. 2).

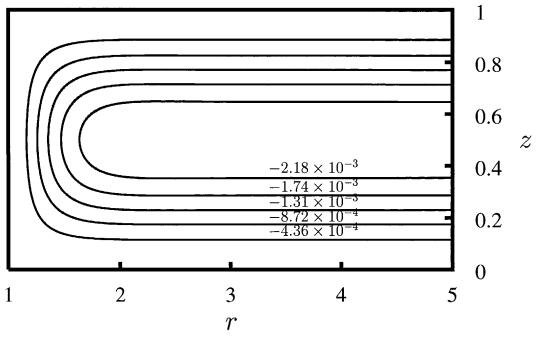

Fig. 3. Leading order stream function $\tilde{\psi}_0^1$ in the hot end region when $\delta = 1$.

The numerical solution to Eq. (91) was obtained using a second order central difference formulation. The matching condition (92) was applied by setting $\tilde{\psi}_0^1 = -(z^4/24 - z^3/12 + z^2/24)$ and $\partial\tilde{\psi}_0^1/\partial r = 0$ at a radius $r = \delta + dr$. Solutions were calculated with $dr = 4$, 6 and 8, and it was observed that the results were insensitive to the choice of dr. All of the numerical solutions discussed in this paper were first calculated using a uniform grid with 201 (radial) by 51 (vertical) nodes and then using a uniform grid with 401 by 101nodes. As discussed below, the key output from the full series of numerical integrations is the value of D_0^3 and this value varied by less than 1.5% when comparing between the two grids.

The energy equation at $O(\lambda^2)$ simplifies to

$$\frac{\partial^2 \tilde{\phi}_0^2}{\partial r^2} + \frac{1}{r}\frac{\partial \tilde{\phi}_0^2}{\partial r} + \frac{\partial^2 \tilde{\phi}_0^2}{\partial z^2} = -\frac{GrPr}{r^2}\frac{\partial \tilde{\psi}_0^1}{\partial z} \tag{93}$$

subject to the boundary conditions $\tilde{\phi}_0^2 = 0$ when $r = \delta$ and $\partial\tilde{\phi}_0^2/\partial z = 0$ when $z = 0, 1$. The matching condition for $\tilde{\phi}_0^2$ is

$$\tilde{\phi}_0^2 \Longleftrightarrow C_0^2 \ln(r/\delta) + D_0^2 + \left(\epsilon^2\hat{\phi}_2^2 + \epsilon^4\hat{\phi}_4^2 + \epsilon^6\hat{\phi}_6^2 + \cdots\right) \tag{94}$$

throughout the intermediate matching region where it is noted that the homogeneous part of the solution $(\tilde{\phi}_0^2)_h = C_0^2 \ln(r/\delta)$ can in fact be neglected since $C_0^2 = 0$. Appendix A lists the functions $\hat{\phi}_{2n}^2$ for $n = 1, 2, 3$.

The value of D_0^2 can be determined by integrating Eq. (93) from $z = 0$, 1 to give

$$\int_0^1 \left(\frac{\partial^2 \tilde{\phi}_0^2}{\partial r^2} + \frac{1}{r}\frac{\partial \tilde{\phi}_0^2}{\partial r} + \frac{\partial^2 \tilde{\phi}_0^2}{\partial z^2}\right) \mathrm{d}z = 0, \tag{95}$$

where it is noted that this equation is valid in the hot end region and throughout the entire intermediate matching region. Since $\tilde{\phi}_0^2 = 0$ when $\delta = 0$, Eq. (95) can be integrated twice with respect to r to give

$$\int_0^1 \tilde{\phi}_0^2 \,\mathrm{d}z = (C_0^2)' \ln(r/\delta), \tag{96}$$

where $(C_0^2)'$ is a numerical constant of integration. Since it can be shown that $\int_0^1 \hat{\phi}_{2n}^2 \, dz = 0$ for all n, substitution of matching condition (94) into Eq. (95) yields $(C_0^2)' = C_0^2$ and more importantly $D_0^2 = 0$. This implies that $C_0^3 = c_0^3 = 0$.

By examining the form of Eqs. (93) and (94), it is seen that $\tilde{\phi}_0^2$ can be decomposed as $\tilde{\phi}_0^2 = GrPr(\tilde{\phi}_0^2)'$ where $(\tilde{\phi}_0^2)'$ satisfies

$$\frac{\partial^2(\tilde{\phi}_0^2)'}{\partial r^2} + \frac{1}{r}\frac{\partial(\tilde{\phi}_0^2)'}{\partial r} + \frac{\partial^2(\tilde{\phi}_0^2)'}{\partial z^2} = -\frac{1}{r^2}\frac{\partial \tilde{\psi}_0^1}{\partial z}. \tag{97}$$

The matching condition for $(\tilde{\phi}_0^2)'$ is obtained from Eq. (94) by setting $C_0^2 = D_0^2 = 0$. As noted in Appendix A $\hat{\phi}_{2n}^2$ can be written as $\hat{\phi}_{2n}^2 = GrPr(\hat{\phi}_{2n}^2)'$ where $(\hat{\phi}_{2n}^2)'$ is independent of Gr and Pr. Eq. (97) was solved using a second order central difference formulation using the same numerical grids which were employed to calculate $\tilde{\psi}_0^1$. During the numerical integration, the sum given in Eq. (94) was truncated at $O(\epsilon^{10})$. The numerically determined solution of Eq. (97) is plotted in Fig. 4 for $\delta = 1$. It is seen that the $O(\lambda^2)$ correction to the temperature field leads to positive perturbations in the top half of the enclosure and negative perturbations in the bottom half of the enclosure.

The vorticity and stream function equations can be combined at $O(\lambda^2)$ to give

$$\left(\frac{\partial^2}{\partial r^2} + \frac{1}{r}\frac{\partial}{\partial r} - \frac{1}{r^2} + \frac{\partial^2}{\partial z^2}\right)\left(\frac{1}{r}\frac{\partial^2}{\partial r^2} - \frac{1}{r^2}\frac{\partial}{\partial r} + \frac{1}{r}\frac{\partial^2}{\partial z^2}\right)\tilde{\psi}_0^2 = -\frac{\partial \tilde{\phi}_0^2}{\partial r} - \frac{Gr}{r}\left(\frac{\partial \tilde{\psi}_0^1}{\partial r}\frac{\partial \tilde{\omega}_0^1}{\partial z} - \frac{\partial \tilde{\psi}_0^1}{\partial z}\frac{\partial \tilde{\omega}_0^1}{\partial r} + \frac{\tilde{\omega}_0^1}{r}\frac{\partial \tilde{\psi}_0^1}{\partial z}\right) \tag{98}$$

with $\tilde{\psi}_0^2 = \partial\tilde{\psi}_0^2/\partial z = 0$ when $z = 0$, 1 and $\tilde{\psi}_0^2 = \partial\tilde{\psi}_0^1/\partial r = 0$ when $r = \delta$. Since it has been shown that $c_0^2 = 0$ and hence that $\hat{\psi}_0^2 = 0$, it follows that the matching condition for $\tilde{\psi}_0^2$ is the sum of the terms in the solutions for $\hat{\psi}_{2n}^2$ which jump to $O(\lambda^2)$ when matching with the hot end region. By examining these core region solutions and by examining Eq. (98) it is seen that $\tilde{\psi}_0^2$ can be decomposed as $\tilde{\psi}_0^2 = GrPr(\tilde{\psi}_0^2)' + Gr(\tilde{\psi}_0^2)''$, where $(\tilde{\psi}_0^2)'$ and $(\tilde{\psi}_0^2)''$ satisfy

$$\left(\frac{\partial^2}{\partial r^2} + \frac{1}{r}\frac{\partial}{\partial r} - \frac{1}{r^2} + \frac{\partial^2}{\partial z^2}\right)\left(\frac{1}{r}\frac{\partial^2}{\partial r^2} - \frac{1}{r^2}\frac{\partial}{\partial r} + \frac{1}{r}\frac{\partial^2}{\partial z^2}\right)(\tilde{\psi}_0^2)' = -\frac{\partial(\tilde{\phi}_0^2)'}{\partial r} \tag{99}$$

and

$$\left(\frac{\partial^2}{\partial r^2} + \frac{1}{r}\frac{\partial}{\partial r} - \frac{1}{r^2} + \frac{\partial^2}{\partial z^2}\right)\left(\frac{1}{r}\frac{\partial^2}{\partial r^2} - \frac{1}{r^2}\frac{\partial}{\partial r} + \frac{1}{r}\frac{\partial^2}{\partial z^2}\right)(\tilde{\psi}_0^2)'' = -\frac{1}{r}\left(\frac{\partial \tilde{\psi}_0^1}{\partial r}\frac{\partial \tilde{\omega}_0^1}{\partial z} - \frac{\partial \tilde{\psi}_0^1}{\partial z}\frac{\partial \tilde{\omega}_0^1}{\partial r} + \frac{\tilde{\omega}_0^1}{r}\frac{\partial \tilde{\psi}_0^1}{\partial z}\right), \tag{100}$$

respectively. The matching conditions for $(\tilde{\psi}_0^2)'$ and $(\tilde{\psi}_0^2)''$ are given by

$$(\tilde{\psi}_0^2)' \Longleftrightarrow \epsilon^2(\hat{\psi}_2^2)' + \epsilon^4(\hat{\psi}_4^2)' + \epsilon^6(\hat{\psi}_6^2)' + \cdots \tag{101}$$

and

$$(\tilde{\psi}_0^2)'' \Longleftrightarrow \epsilon^2(\hat{\psi}_2^2)'' + \epsilon^4(\hat{\psi}_4^2)'' + \epsilon^6(\hat{\psi}_6^2)'' + \cdots, \tag{102}$$

where it is noted that $(\hat{\psi}_{2n}^2)'$ and $(\hat{\psi}_{2n}^2)''$ are listed in Appendix A for $n = 1, 2, 3$. The solution of Eqs. (99) and (100) subject to the appropriate boundary and matching conditions have been obtained numerically and the results for the specific value of $\delta = 1$ are plotted in Fig. 5 where it is noted that the summations in Eqs. (101) and (102) were truncated at $O(\epsilon^{10})$. It is seen that the $(\tilde{\psi}_0^2)'$ perturbation consists of 4 counter-rotating cells with two of the cells confined near the inner cylinder and the other two cells extending into the intermediate matching region. The $(\tilde{\psi}_0^2)''$ perturbation consists of two counter-rotating cells which only extend a short distance from the inner cylinder.

The energy equation at $O(\lambda^3)$ in the hot end region is given by

$$\frac{\partial^2 \tilde{\phi}_0^3}{\partial r^2} + \frac{1}{r}\frac{\partial \tilde{\phi}_0^3}{\partial r} + \frac{\partial^2 \tilde{\phi}_0^3}{\partial z^2} = \frac{GrPr}{r}\left(\frac{\partial \tilde{\psi}_0^1}{\partial r}\frac{\partial \tilde{\phi}_0^2}{\partial z} - \frac{\partial \tilde{\psi}_0^1}{\partial z}\frac{\partial \tilde{\phi}_0^2}{\partial r}\right) - \frac{GrPr}{r^2}\frac{\partial \tilde{\psi}_0^2}{\partial z}, \tag{103}$$

subject to the boundary conditions $\tilde{\phi}_0^3 = 0$ when $r = \delta$ and $\partial\tilde{\phi}_0^3/\partial z = 0$ when $z = 0, 1$. The matching condition for $\tilde{\phi}_0^3$

$$\tilde{\phi}_0^3 \Longleftrightarrow D_0^3 + \epsilon^2\hat{\phi}_2^3 + \epsilon^4\hat{\phi}_4^3 + \epsilon^6\hat{\phi}_6^3 + \cdots, \tag{104}$$

where it is noted that previous matching has shown that $C_0^3 = c_0^3 = 0$ so that the homogeneous solution $(\tilde{\phi}_0^3)_h$ vanishes. The $\hat{\phi}_{2n}^3$ terms represent core region solutions which jump order when matching with the hot end region. The matching condition and Eq. (103) are such

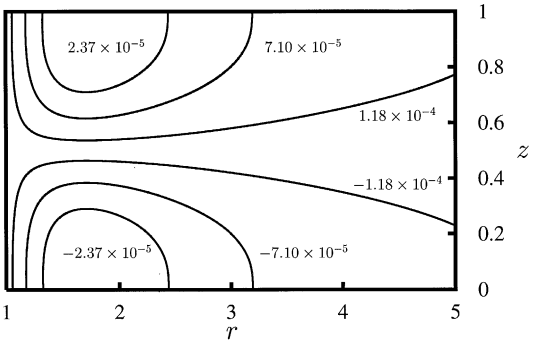

Fig. 4. The $O(\lambda^2)$ temperature perturbation $\tilde{\phi}_0^2$ in the hot end region when $\delta = 1$.

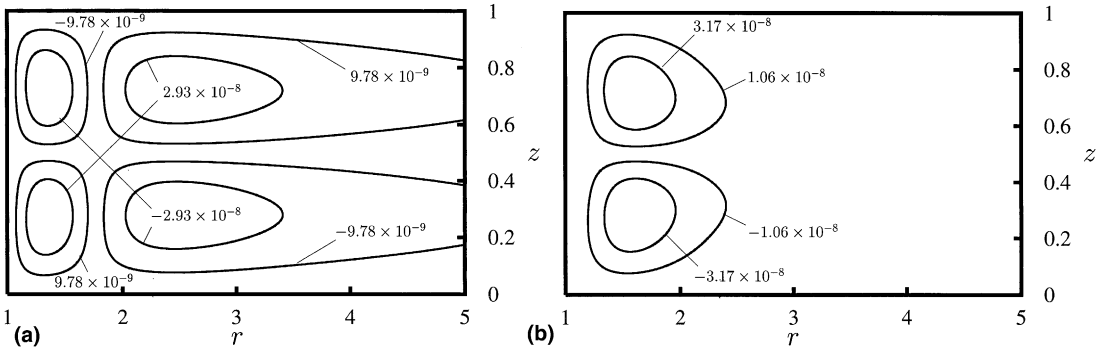

Fig. 5. The $O(\lambda^2)$ stream function perturbation in the hot end region when $\delta = 1$: (a) $(\tilde{\psi}_2^2)'$; (b) $(\tilde{\psi}_2^2)''$.

that $\tilde{\phi}_0^3$ can be decomposed as $\tilde{\phi}_0^3 = (GrPr)^2(\tilde{\phi}_0^3)' + (Gr^2Pr)(\tilde{\phi}_0^3)''$, where $(\tilde{\phi}_0^3)'$ and $(\tilde{\phi}_0^3)''$ satisfy

$$\frac{\partial^2(\tilde{\phi}_0^3)'}{\partial r^2} + \frac{1}{r}\frac{\partial(\tilde{\phi}_0^3)'}{\partial r} + \frac{\partial^2(\tilde{\phi}_0^3)'}{\partial z^2} = \frac{1}{r}\left(\frac{\partial\tilde{\psi}_0^1}{\partial r}\frac{\partial(\tilde{\phi}_0^2)'}{\partial z} - \frac{\partial\tilde{\psi}_0^1}{\partial z}\frac{\partial(\tilde{\phi}_0^2)'}{\partial r}\right) - \frac{1}{r^2}\frac{\partial(\tilde{\psi}_0^2)'}{\partial z} \tag{105}$$

and

$$\frac{\partial^2(\tilde{\phi}_0^3)''}{\partial r^2} + \frac{1}{r}\frac{\partial(\tilde{\phi}_0^3)''}{\partial r} + \frac{\partial^2(\tilde{\phi}_0^3)''}{\partial z^2} = -\frac{1}{r^2}\frac{\partial(\tilde{\psi}_0^2)''}{\partial z}, \tag{106}$$

respectively. The matching conditions for $(\tilde{\phi}_0^3)'$ is

$$(\tilde{\phi}_0^3)' \Longleftrightarrow (D_0^3)' + \epsilon^2(\hat{\phi}_2^3)' + \epsilon^4(\hat{\phi}_4^3)' + \epsilon^6(\hat{\phi}_6^3)' + \cdots \tag{107}$$

and the matching conditions for $(\tilde{\phi}_0^3)''$ is

$$(\tilde{\phi}_0^3)'' \Longleftrightarrow (D_0^3)'' + \epsilon^2(\hat{\phi}_2^3)'' + \epsilon^4(\hat{\phi}_4^3)'' + \epsilon^6(\hat{\phi}_6^3)'' + \cdots, \tag{108}$$

where it is noted that $D_0^3 = (GrPr)^2(D_0^3)' + (Gr^2Pr)(D_0^3)''$ and that $(\hat{\phi}_{2n}^3)'$ and $(\hat{\phi}_{2n}^3)''$ are listed in Appendix A for $n = 1, 2, 3$.

Following CLI, the unknown constant $(D_0^3)'$ is determined as part of the solutions to Eq. (105). In particular matching condition (107) is replaced by

$$\frac{\partial(\tilde{\phi}_0^3)'}{\partial r} = \frac{\partial}{\partial r}\left(\epsilon^2(\hat{\phi}_2^3)' + \epsilon^4(\hat{\phi}_4^3)' + \epsilon^6(\hat{\phi}_6^3)' + \cdots\right) \tag{109}$$

and the value of $(D_0^3)'$ is determined from the numerical solutions of Eq. (105) by defining

$$(\Delta_0^3)' = (\tilde{\phi}_0^3)' - (\epsilon^2(\hat{\phi}_2^3)' + \epsilon^4(\hat{\phi}_4^3)' + \epsilon^6(\hat{\phi}_6^3)' + \cdots) \tag{110}$$

and then examining the value of $(\Delta_0^3)'$ throughout the intermediate matching region. In the numerical implementation the summations in Eqs. (109) and (110) were truncated at $O(\epsilon^{10})$. The value of $(D_0^3)''$ is determined using the same procedure which led to Eqs. (95) and (96). This gives $(D_0^3)'' = 0$ for all δ.

The numerical solution for $(\tilde{\phi}_0^3)'$ when $\delta = 1$ was used to generate the plot of $(\Delta_0^3)'$ in Fig. 6. The solid curve corresponds to the maximum value of $(\Delta_0^3)'$ over the interval $0 \leqslant z \leqslant 1$ as a function of r while the dashed curve corresponds to the minimum value. It is seen that $(D_0^3)'$ approaches a constant value of $(D_0^3)' = -5.7 \times 10^{-7}$ in the intermediate matching region. Thus $D_0^3 = (GrPr)^2 \times (D_0^3)'$ is the first nonzero value of D_0^k and this term forces the first convective contribution to the core region solutions at $O(\lambda^4)$ since $c_0^4 = D_0^3$. For completeness $(\tilde{\phi}_0^3)''$ is plotted in Fig. 7 for $\delta = 1$. This temperature perturbation is symmetric about the plane $z = 1/2$ with the perturbation rapidly decaying as r extends into the intermediate matching region.

In principle, it is possible at this point to continue to higher orders in λ to determine values of D_0^k for $k > 3$. To do so, however, would require the numerical solution of an ever increasing number of equations. Since the effort required to solve these equations in the hot end region is in effect comparable to the effort which would be required to solve the full nonlinear equations for convection in the entire annular enclosure, it has been

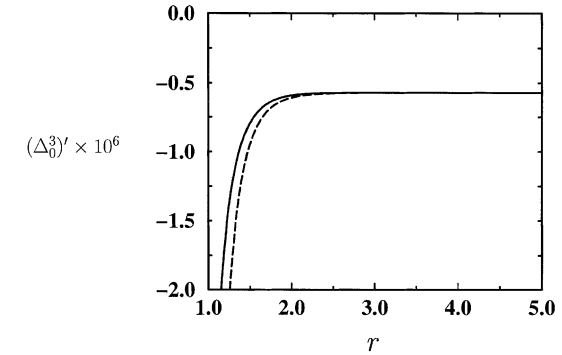

Fig. 6. The maximum (solid line) and minimum (dashed line) of $(\Delta_0^3)'$ as a function of r when $\delta = 1$.

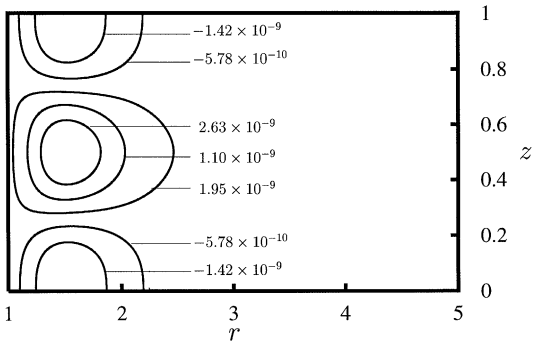

Fig. 7. The $O(Gr^2Pr\lambda^3)$ temperature perturbation $(\tilde{\phi}_0^3)''$ in the hot end region when $\delta = 1$.

decided to terminate the asymptotic analysis at $O(\lambda^3)$. By not proceeding beyond $O(\lambda^3)$ in the hot end region, the asymptotic solutions in the core region are only completely specified to $O(\lambda^4)$.

4.4. The influence of varying δ

The results presented in Fig. 6 show that D_0^3 is non-zero for the specific value of $\delta = 1$. In order to show how D_0^3 varies as a function of δ the numerical integrations described above were repeated for values of δ between 0.1 and 10. The results are shown in Fig. 8 which plots $(D_0^3)'$ a function of δ where it is recalled that $D_0^3 = (GrPr)^2(D_0^3)'$. Fig. 8 shows that $(D_0^3)'$ is a decreasing functions of δ. For a fixed (but small) value of ϵ, the asymptotic solutions for the case when δ is of $O(1)$ should approach the asymptotic solutions for the case when Γ is of $O(1)$ when δ becomes sufficiently large and Γ becomes sufficiently small. Since the first convective contribution in the core region occurs at $O(\epsilon^2)$ for the case when Γ is of $O(1)$, it follows that the $O(\lambda^4)$ convective contribution in the core region for the case when δ is of $O(1)$ must vanish for large δ. This is indeed consistent with the results plotted in Fig. 8.

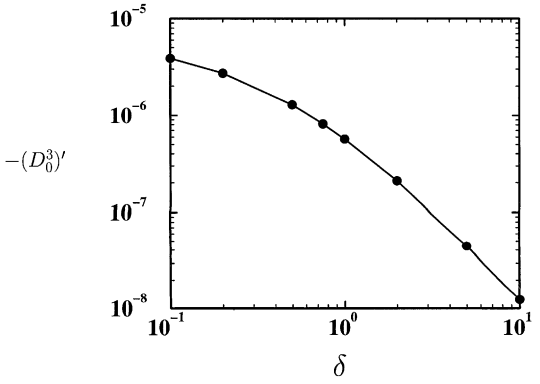

Fig. 8. The variation of $(D_0^3)'$ with δ.

5. Nusselt number

A fundamental quantity when examining natural convection within enclosures is the Nusselt number, Nu, which represents the ratio of the total rate of heat transfer to some relevant conduction heat transfer scale. For convection in the annular gaps considered here it is the radial heat transfer between the inner and outer cylinder which is of interest and Nu is defined as

$$Nu = \frac{q^*_{\text{total}}}{2\pi h r_1 k(T_1 - T_2)/\ell}, \tag{111}$$

where q^*_{total} is the integrated radial heat transfer through any concentric cylindrical shell between the inner and outer cylinder and k is the thermal conductivity of the fluid in the annular cavity. In terms of the nondimensional variables defined in Eq. (5) the Nusselt number is evaluated as

$$Nu = \frac{r'}{\Gamma}\int_0^1 \left(GrPr\epsilon u\theta - \frac{\partial\theta}{\partial r}\right)|_{r=r'}\,\mathrm{d}z, \tag{112}$$

where $\delta \leqslant r' \leqslant \delta + 1/\epsilon$. Note that global conservation of energy implies that Nu is independent of the choice of r' used in Eq. (112).

For the case when $\epsilon \to 0$ with Γ is of $O(1)$ the core region solutions can be substituted into Eq. (112) to give

$$Nu = \frac{1}{\Gamma\ln((\Gamma+1)/\Gamma)} + \epsilon^2\frac{(GrPr)^2}{725\,760}\frac{2\Gamma+1}{\Gamma^3(\Gamma+1)^2} \times \frac{1}{(\ln((\Gamma+1)/\Gamma))^4} + O(\epsilon^3). \tag{113}$$

In the limit as $\Gamma \to \infty$ Eq. (113) approaches the corresponding result obtained by CLI for convection in shallow rectangular enclosures which is given by $Nu = 1 + (\epsilon GrPr)^2/362\,880$.

For the case when $\epsilon \to 0$ with δ is of $O(1)$ the core region solutions can be substituted into Eq. (112) to give

$$Nu = -\frac{1}{\Gamma}\left(\lambda + c_0^4\lambda^4\right) + O(\lambda^5), \tag{114}$$

where it is noted that the asymptotic parameter λ is negative with $\lambda = -1/\ln((\Gamma+1)/\Gamma)$. The quantity c_0^4 in Eq. (114) is a function of δ with $c_0^4 = (D_0^3)'(GrPr)^2$.

A detailed parametric study of Nu as a function of Gr, ϵ and δ has been performed [7] and the results indicate that the correlations given by Eqs. (113) and (114) are only appropriate when $GrPr\epsilon \leqslant 400$.

6. Summary

This paper has presented asymptotic solutions for convection in shallow cylindrical annuli in the limit as the aspect ratio $\epsilon \to 0$. A key feature of the asymptotic

analysis is that the solutions at $O(\epsilon^n)$ can only be completely determined by examining the governing equations at $O(\epsilon^{n+2})$. The asymptotic analysis was performed for the case when $\epsilon \to 0$ with Γ of O(1) and for the case $\epsilon \to 0$ with δ of O(1). The analysis involved matching solutions in the end regions near the inner and outer cylinders with solutions in a central core region. When $\epsilon \to 0$ with δ of O(1) the asymptotic analysis is considerably complicated by the fact that terms in the core region solutions jump order when matching with solutions in the hot end region. It has been shown that curvature effects dramatically dictate the order at which convection influences the core region solutions (i.e., there is a Gr number dependence). When $\epsilon \to 0$ with Γ of O(1) the first convective influence in the core region occurs at $O(\epsilon^2)$. When $\epsilon \to 0$ with δ of O(1) the first convective influence in the core region occurs at $O(\lambda^4)$ where $\lambda = 1/\ln(\epsilon\delta/(1+\epsilon\delta))$, while small, is a much larger asymptotic parameter than ϵ as $\epsilon \to 0$. Thus the asymptotic solutions are fundamentally different when $\epsilon \to 0$ with Γ of O(1) and when $\epsilon \to 0$ with δ of O(1).

Appendix A. Higher order solutions when δ is of O(1)

For all $n > 1$ there are terms in the core region solutions at $O(\epsilon^{2n})$ which jump to O(1) when matching with the hot end region solutions when δ is of O(1). This appendix lists the terms in the core region solutions for $\hat{\phi}^2_{2n}$, $\hat{\psi}^2_{2n}$ and $\hat{\phi}^3_{2n}$ which jump order for $n = 1, 2, 3$. These solutions are obtained following the same procedure detailed in Section 3.1 for the case when when $\Gamma = O(1)$. The solutions listed here omit the homogeneous terms in the core region solutions (such as the $c_2^k \ln \hat{r} + d_2^k$ term in Eq. (79)) which do not jump to O(1) when matching with the hot end region.

The terms which jump order for the temperature field at $O(\epsilon^{2n}\lambda^2)$ can be decomposed as

$$\hat{\phi}^2_{2n} = GrPr(\hat{\phi}^2_{2n})', \tag{115}$$

where

$$(\hat{\phi}^2_2)' = (12z^5 - 30z^4 + 20z^3 - 1)/1440\hat{r}^2, \tag{116}$$

$$(\hat{\phi}^2_4)' = -(8z^7 - 28z^6 + 28z^5 - 14z^2 + 3)/10\,080\hat{r}^4 \tag{117}$$

and

$$(\hat{\phi}^2_6)' = (4z^9 - 18z^8 + 24z^7 - 42z^4 + 54z^2 - 11)/22\,680\hat{r}^6. \tag{118}$$

The terms which jump order for the stream function field at $O(\epsilon^{2n}\lambda^2)$ can be decomposed as

$$\hat{\psi}^2_{2n} = GrPr(\hat{\psi}^2_{2n})' + Gr(\hat{\psi}^2_{2n})'', \tag{119}$$

where

$$(\hat{\psi}^2_2)' = (2z^7 - 9z^6 + 12z^5 - 21z^2 + 22z - 6)z^2/362\,880\hat{r}^2, \tag{120}$$

$$(\hat{\psi}^2_4)' = -(12z^9 - 66z^8 + 110z^7 - 462z^4 + 484z^3 + 275z^2 - 504z + 151)z^2/9\,979\,200\hat{r}^4, \tag{121}$$

$$(\hat{\psi}^2_6)' = (280z^{11} - 1820z^{10} + 3640z^9 - 30\,030z^6 + 31\,460z^5 + 70\,070z^4 - 91\,728z^3 - 45\,955z^2 + 92\,054z - 27\,971)z^2/756\,756\,000\hat{r}^6, \tag{122}$$

$$(\hat{\psi}^2_2)'' = (10z^6 - 45z^5 + 78z^4 - 63z^3 + 21z^2 - 1)z^3/181\,440\hat{r}^2, \tag{123}$$

$$(\hat{\psi}^2_4)'' = -(120z^9 - 660z^8 + 1430z^7 - 1485z^6 + 660z^5 - 66z^3 - 2z + 3)z^2/14\,968\,800\hat{r}^4 \tag{124}$$

and

$$(\hat{\psi}^2_6)'' = (2100z^{11} - 13\,650z^{10} + 35\,490z^9 - 45\,045z^8 + 25\,025z^7 - 4290z^5 - 364z^3 + 910z^2 - 103z - 73)z^2/1\,135\,134\,000\hat{r}^6. \tag{125}$$

The terms which jump order for the temperature field at $O(\epsilon^{2n}\lambda^3)$ can be decomposed as

$$\hat{\phi}^3_{2n} = (GrPr)^2(\hat{\phi}^2_{2n})' + (Gr^2Pr)(\hat{\phi}^2_{2n})'', \tag{126}$$

where

$$(\hat{\phi}^3_2)' = 1/725\,760\hat{r}^2, \tag{127}$$

$$(\hat{\phi}^3_4)' = -(15\,048z^{10} - 75\,240z^9 + 142\,560z^8 - 118\,800z^7 + 36\,960z^6 - 11\,088z^5 + 21\,120z^4 - 11\,880z^3 + 1320z^2 - 91)/479\,001\,600\hat{r}^4, \tag{128}$$

$$(\hat{\phi}^3_6)' = (3\,882\,060z^{12} - 23\,292\,360z^{11} + 53\,153\,100z^{10} - 52\,252\,200z^9 + 18\,918\,900z^8 - 18\,378\,360z^7 + 38\,198\,160z^6 - 13\,513\,500z^5 - 16\,551\,990z^4 + 10\,581\,480z^3 - 745\,290z^2 + 84\,173)/490\,377\,888\,000\hat{r}^6, \tag{129}$$

$$(\hat{\phi}^3_2)'' = 0, \tag{130}$$

$$(\hat{\phi}^3_4)'' = -(1320z^{10} - 6600z^9 + 12\,870z^8 - 11\,880z^7 + 4620z^6 - 330z^4 + 1)/239\,500\,800\hat{r}^4 \tag{131}$$

and

$$(\hat{\phi}_6^3)'' = (36\,400z^{12} - 218\,400z^{11} + 520\,520z^{10} - 600\,600z^9 + 300\,300z^8 - 40\,040z^6 - 910z^4 + 1820z^3 + 910z^2 - 83)/27\,243\,216\,000\hat{r}^6. \quad (132)$$

References

[1] D.E. Cormack, L.G. Leal, J. Imberger, Natural convection in a shallow cavity with differentially heated end walls. Part 1. Asymptotic theory, J. Fluid Mech. 65 (1974) 209–229.

[2] D.E. Cormack, L.G. Leal, J.H. Sienfield, Natural convection in a shallow cavity with differentially heated end walls. Part 2. Numerical solutions, J. Fluid Mech. 65 (1974) 231–246.

[3] J. Imberger, Natural convection in a shallow cavity with differentially heated end walls. Part 3. Experimental results, J. Fluid Mech. 65 (1974) 247–260.

[4] G. de Vahl Davis, R. Thomas, Natural convection between concentric vertical cylinders, Phys. Fluids. (1969) 198–207 (Suppl. II).

[5] G.P. Merker, L.G. Leal, Natural convection in a shallow annular cavity, Int. J. Heat Mass Transfer 23 (1980) 677–686.

[6] E.J. Hinch, Perturbation Methods, Cambridge University Press, Cambridge, 1991.

[7] D.M. Leppinen, Aspects of convection, Ph.D. Thesis, University of Cambridge, Cambridge, 1997.